PROBING GAS-PHASE DYNAMICS WITH PICOSECOND TRANSIENT GRATING SPECTROSCOPY

Todd S. ROSE and M.D FAYER

Department of Chemistry, Stanford University, Stanford, CA 94305, USA

Received 28 December 1984; in final form 5 February 1985

The application of the transient grating method to the understanding of gas-phase velocity distributions and collisional effects is presented. Theoretical models are discussed in view of the experimental data obtained from iodine vapor. Applications of the transient grating method to other gas-phase problems are also mentioned.

1. Introduction

A novel approach to the study of gas-phase dynamics, e.g., velocity distributions and collisional effects [1], involves the application of the transient grating method [2]. In the simplest case, where there are no collisions on the time scale of the experiment, the signal is the Fourier transform of the velocity distribution. However, in the experiments on I_2 presented below, state-changing collisions are observed. Therefore, it is necessary to consider the effect of these collisions as well as the velocity distribution in the analysis of the signal. In addition, it should be possible with this technique to investigate the velocities of photofragments and the influence of vibronic energy on collisional events as well as other problems in which knowledge of the velocity distribution is essential.

There is a wide variety of experiments used to probe velocity and collisional effects [3,4]. Brewer and co-workers [3] employed photon echoes to study grazing collisions. A single vibration–rotation line was excited with a narrow band laser. The time dependence of the photon echo signal revealed information on the velocity changes produced by collisions which preserved the vibration–rotation state. There is quantitative agreement between experiment and theory which provides considerable insight into the effects of grazing collisions. Warren [5] is currently using narrow band pump–probe experiments to examine velocity changing collisions. In these experiments, a narrow band dye laser is tuned to a frequency in the Doppler profile of a single ro-vibronic transition. A second dye laser probes the time-dependent bleaching at a second frequency in the line. By using pulse sequences with various phases one can obtain various types of information on collisionally induced velocity changes. In these experiments, as well as those which measure Doppler linewidths in equilibrium [6,7] or chemically reacting systems [7], information on velocity and collisions is obtained in some manner from the narrow frequency band width of the experiment.

The grating approach is inherently different. It examines the spatial position of molecules as a function of time, and thereby obtains velocity information. The measurement of gas-phase velocity distributions is analogous to recent grating experiments used to examine exciton transport in crystals [8,9]. It works in the following manner (see fig. 1). Two time-coincident picosecond laser pulses of the same wavelength are crossed in the sample. Interference between the two coherently related pulses creates an optical fringe pattern in the sample such that the intensity of light varies sinusoidally in the beam overlap region. The interference fringe spacing is determined by the angle between the beams and by the wavelength of the light.

When the frequency of the excitation pulses coincides with an absorption band of the gas-phase molecule, excited states are produced. These excitations initially will have the same spatial distribution as the

0 009-2614/85/$ 03.30

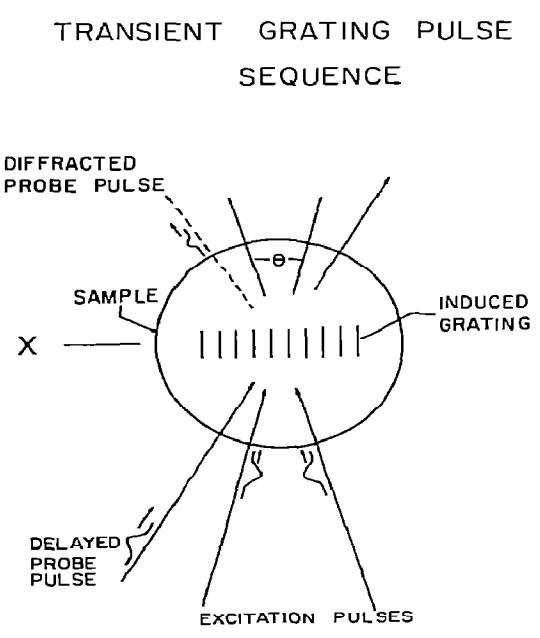

Fig. 1. Schematic illustration of the transient grating experiment. Two coherently related pulses crossed in the sample yield a spatially sinusoidally varying concentration of excited states. This acts as a diffraction grating for the variably delayed probe pulse. The signal is the intensity of the diffracted probe versus probe delay time.

sinusoidal optical interference pattern, i.e. there will be an oscillatory variation in the concentration of excited states. After a suitable time delay, a probe pulse (which may differ in wavelength from the excitation pulses) is directed into the sample along a third path. The probe pulse experiences an inhomogeneous optical medium resulting from the alternating regions of high and low concentrations of excited states. These alternating regions have different indices of refraction, and consequently, a periodic variation in the index of refraction is established. Thus, the probe pulse encounters a grating which causes it to diffract into one or more orders (see fig. 1).

Now consider the effect of the translational motion of the excited gas-phase molecules. These excited molecules will move from regions of high excited state concentration, grating peaks, to areas of low excited state concentration, grating nulls. Thus, the translational motion will fill in the grating nulls and deplete the peaks. Destruction of the grating pattern by spatial redistribution of the excited molecules leads to a decrease in the intensity of the diffracted probe pulse as the probe delay time is increased [10]. Thus, the time dependence of the grating signal is directly determined by the translational motion.

In the experiments described below, the grating signal was not only found to be sensitive to the motions of the molecules, but also to collisionally induced state changes. This resulted from the fact that the probe was tuned to a wavelength that was sensitive to a state populated by collisions.

2. Mathematical formulation

Consider a gas to be in thermal equilibrium at temperature T and to have velocity distribution given by

$$f(V_x) = (m/2\pi k_B T)^{1/2} \exp(-mV_x^2/2k_B T). \quad (1)$$

x is the grating wave vector direction (see fig. 1). Since the grating fringe spacing (1–15 μm) is much smaller than the other dimensions in the problem (grating height and depth are hundreds of μm) only the motion in the x direction will influence the signal.

At time $t = 0$ the relative concentration of excited molecules at position x is

$$N(x, 0) = \tfrac{1}{2}(\cos \Delta x + 1), \quad (2)$$

where $\Delta = 2\pi/d$ and the fringe spacing $d = \lambda/2 \sin(\theta/2)$ [8]. λ is the wavelength of the excitation beams and θ is the angle between them (see fig. 1). We need to calculate the difference in the excited concentration of the grating peaks and nulls at time t, to determine the signal $S(t)$. At any position x, the relative concentration of excited molecules with velocity V_x in the absence of collisions is

$$N^V(x, t) = \tfrac{1}{2}\{\cos[\Delta(x + V_x t)] + 1\} f(V_x). \quad (3)$$

To evaluate the peak – null difference in excited state concentration we need $N(x, t)$,

$$N(x, t) = \int_{-\infty}^{\infty} N^V(x, t)\, \mathrm{d}V_x. \quad (4)$$

The signal, $S(t)$, is proportional to $D^2(t)$,

$$S(t) = AD^2(t) = A\,[N(0, t) - N(d/2, t)]^2. \quad (5)$$

Substituting eq. (3) into eq. (4) and then substi-

tuting this result into eq. (5) yields

$$S(t) = A\left(\int_{-\infty}^{\infty} f(V_x)\cos(\Delta V_x t)\,\mathrm{d}V_x\right)^2. \quad (6)$$

For a velocity distribution described by eq. (1), eq. (6) becomes

$$S(t) = A\,\exp[-(\Delta t)^2 k_B T/m]. \quad (7)$$

Eq. (7) shows that a Gaussian velocity distribution yields a signal which is Gaussian in time. In general, if the experiment is performed fast on the time scale of collisions, the signal is the Fourier transform of the velocity distribution as shown by eq. (6). By changing Δ (changing the fringe spacing) one can scale the time such that different portions of the velocity distribution are emphasized.

In the experiments described below, it will be demonstrated that only molecules which are involved in state-changing collisions are probed. This occurs because the wavelength of the probe is strongly absorbed by molecules in the final state populated by collisions but negligibly absorbed by molecules in the initial state. Thus, the experiment probes collisional dynamics as well as the velocity distribution of the initial and final states. Model calculations will be described in connection with the data in section 4. The mathematical details are too lengthy to present here and will be given elsewhere. A zeroth-order model, but one that is qualitatively correct, takes the population build up in the final state to be exponential and writes the signal as a product of the grating decay due to the molecular motion (velocity) and the observable grating build-up due to final state population growth,

$$S(t) = A\,\exp[-(\Delta t)^2 k_B T/m]\,[1 - \exp(-kt)]. \quad (8)$$

In eq. (8) k is related to the collision cross section for populating the observed state from the initial state. For very large fringe spacings, the Gaussian term is constant over the time scale of the experiment, and the signal grows in exponentially as the observed state is populated by collisions. At smaller fringe spacing, the Gaussian decay caused by destruction of the grating spatial pattern by molecular motion, competes with the exponential growth. Eq. (8) is useful because it permits the grating fringe spacing dependence of the data presented below to be understood qualitatively. It is not an accurate description because it does not properly account for the location of a molecule at the time of collision, nor does it permit, for example, the velocity distribution of molecules in the observed state to be different from the distribution in the initial state. The model calculations, presented in section 4, include the essential details.

3. Experimental procedures

The experimental apparatus is described in detail elsewhere [10]. The doubled output of an actively mode-locked and Q-switched Nd : YAG laser is used to synchronously pump a dye laser. The tunable 50 ps 10 μJ dye pulse is beam split and the resulting two pulses are crossed to form the grating. In these experiments the excitation is at 560 nm. The probe pulse is a single 532 nm, 100 ps, 5 μJ doubled Nd : YAG pulse. The excitation pulses have a band width of $\approx$10 cm^{-1} while the probe pulse has a band width of $\approx$1/3 cm^{-1}. A motorized delay line is used to obtain up to 16 ns delay. A phototube, lock-in amplifier, and computer are used to record the diffracted signal as a function of time (delay line position).

The sample is I_2 vapor in a 1 cm path length evacuated cell. The temperature of the cell is held at 248 K and monitored with a resistance thermometer in contact with the cell face. In the experiments the I_2 pressure is maintained at approximately 16 Torr by controlling the temperature of a side arm on the cell.

4. Results and discussion

Fig. 2 shows transient grating data taken with a large (15 μm) fringe spacing. The signal is seen to have $\approx$0 intensity at $t = 0$ and to grow rapidly with time. The 560 nm excitation wavelength causes transitions from the ground X state to $v \approx 19$ vibrational level of the B state [11,12]. The 532 nm probe corresponds to a transition from the X state to $v \approx 31$ of the B state [11,12]. In the absence of collisionally induced state changes, the probe should experience a maximum variation in the optical density at $t = 0$ resulting from the depletion of the ground-state molecules in the nulls by the crossed excitation beams. This should result in a signal that is a maximum at $t = 0$. Also, the absorption arising from the X $\rightarrow$ 532 nm transition is

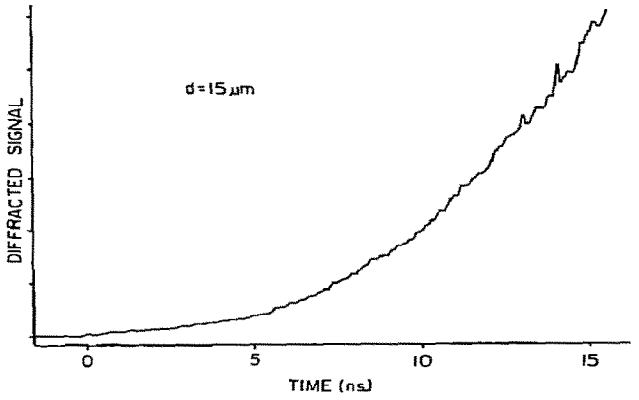

Fig. 2 The experimental curve was obtained with a fringe spacing of 15 μm. At large fringe spacings the decay of the grating resulting from molecular motion is minimal on the experimental time scale. Only a buildup of population in the observable state contributes to the time dependence of the signal.

weak [13], and should give rise to a very weak signal [10].

The fact that a strong increasing signal is observed demonstrates that the state being probed is not the initially prepared excited state. At the temperature and pressure of the experiment, there are a small number of collisions (<10) during the time of the experiment. These collisions must cause state changes to another electronic state or to a different region of the vibrational manifold of the B state. The new state formed cannot be a dissociative state since the rising signal implies a build-up of population. Furthermore, iodine atoms do not absorb the 532 nm probe.

Fig. 3 illustrates the observed fringe spacing dependence. Except for differing fringe spacings, the conditions for each data set are identical. As the fringe spacing is decreased, the destruction of grating pattern by the molecular motion becomes increasingly important. The rapid rise in signal is damped by the Gaussian decay produced by the distribution of molecular velocities. This is the qualitative behavior shown by eq. (8).

To obtain a better understanding of the system dynamics which give rise to the time dependence and fringe spacing dependence of fig. 3, we present two basic models for the state-changing collision process. First we consider cases in which a *single collision*

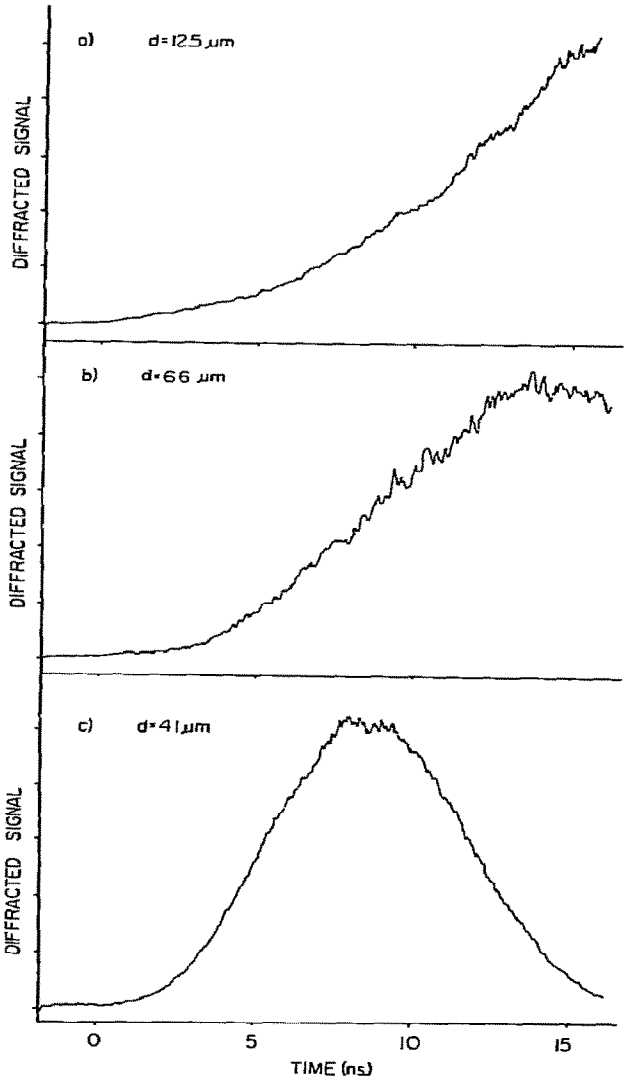

Fig. 3. Fringe spacing dependence of the grating signal. As the fringe spacing is decreased the influence of the molecular motion becomes more apparent. At smaller fringe spacings the grating is destroyed at earlier times; hence, the signal peaks earlier. The sample temperature and pressure for all three curves are 248 K and 16 Torr.

takes a molecule from the initial state to the observed state. For all variations of this model it is possible to qualitatively reproduce the fringe spacing dependence. However, as shown in fig. 4a, the detailed shapes of the curves are not correct.

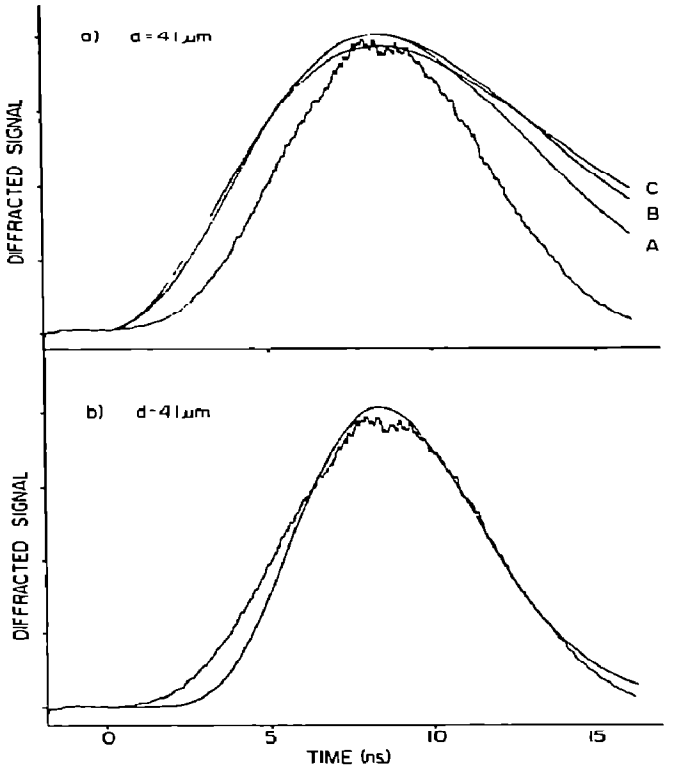

Fig. 4. (a) Calculated curves for the single-step collision models are compared to the data. Curves A and B are derived from a model which randomizes the initial velocity of each molecule into a Gaussian distribution after one collision. The initial temperature is 428 K while the final temperatures are 150 and 80 K, and the collision parameters are 2.3 and 5.0 Å for curves A and B, respectively. Curve C is an opposite limiting case in which the initial velocity of each molecule is unchanged by collision. Both A and C have velocity-independent collision rate constants, while that of B is velocity dependent. (b) Calculated curve for the multistep collision model. The excited molecules undergo a random walk in energy space. The collision parameter is 5 Å (approximately hard sphere) and the temperature is the sample temperature. Comparison of the curves in (a) and (b) indicates that the multistep collision model gives better agreement with the data.

Curve A is calculated with a velocity-independent collision rate constant (i.e. the collision constant for each molecule in the velocity distribution is given the ensemble average constant). The velocity of each molecule is assumed to randomize after a single collision. The final velocity distribution in the observable state is Maxwell–Boltzmann, but it can have a different temperature than the temperature of the initial state (i.e. the temperature of the sample cell). Curve A is the best fit with this model. It uses an effective collision parameter of 2.3 Å and a final distribution temperature of 153 K. Note that while the peak position is correct, the curve is much too broad. Curve B is derived from premises similar to curve A, but now a velocity-dependent collision rate is used. The collision rate depends on the velocity of the particular molecule, rather than an average speed. The final temperature and collision parameter are 80 K and 5.0 Å, respectively. Again the calculated curve is much too broad.

Curve C is an opposite limiting case. In the model which produces curves A and B, the velocity of each colliding molecule is Gaussian distributed after a single collision. In the model for curve C the velocity of each molecule is assumed to be unchanged by a collision. Curve C is the best fit for this model. The collision parameter is 6.1 Å and since the velocity is unchanged on collision, the final temperature is set equal to the initial temperature. The collision rate was taken to be velocity independent as for curve A. Similar results are obtained when the collision rate is made velocity dependent. In all the cases examined (for single-step processes) qualitatively correct fringe spacing dependences and plausible fitting parameters are obtained, but quantitative agreement is lacking.

In fig. 4b we show the results of a calculation in which it is assumed that a multistep process takes the system from the initial state to the observable state. In this model an excited molecule undergoes a random walk in energy space. For the calculation in fig. 4b, the initial and final temperatures are set equal to the experimental temperature and an approximate hard-sphere collision parameter of 5 Å is used. It is assumed that a migration in energy space over a distance of ΔE must occur in order to reach the observable state. This is a multistep process. There is one adjustable parameter if the temperature and cross section are chosen as above. The adjustable parameter, which we will call R, is the ratio of ΔE to the random walk energy step size.

It is seen from figs. 4a and 4b that the agreement between theory and experiment is greatly improved when the multistep process, as opposed to the single-step process, is employed. Not only does the 4b calculated curve show better agreement with the data, but also the parameters involved are more reasonable.

In the calculation of curves A and B (fig. 4a) final temperatures which are quite low were necessary to fit the data. Furthermore, the collision parameter used in the calculation in 4b was chosen to be the I_2 hard-sphere parameter, i.e. approximately 5.3 Å [14]. Since there are only a small number of collisions during the experiment, the number of steps in the walk must be small. R is related qualitatively to the number of steps in the walk. For the multistep model to be reasonable, R must be on the order of unity since there are only a small number of collisions during the experiment. The curve shown in fig. 4b has $R = 1$. One possible scenario for this multistep model is that collisions induce changes in the vibrational state within the B manifold. Population of certain vibrational states (perhaps those near bottom of the B state where mixing with dissociative states could provide oscillator strength for the absorption at 532 nm) could result in the build up of signal illustrated in figs. 2 and 3.

5. Concluding remarks

We have presented a new approach to the investigation of gas-phase velocity distributions and collisional processes which employs a picosecond transient grating technique It was demonstrated that I_2 molecules excited to the electronic B state and vibrational state $v \approx 19$, undergo state changing collisions which populate another state with strong absorption at 532 nm. The identity of this state is uncertain. The comparison of the data to dynamical models of the experiment suggest that multiple collisions are required to populate the state observed in the experiment. We will perform additional experiments at other I_2 pressures and with rare gas buffers. These experiments will improve our understanding of the processes being observed in the I_2 system.

The general approach described here can be useful in a number of contexts. For example, if the grating excitation causes photofragmentation, the probe (tuned to a fragment absorption) will measure the photofragment velocity distribution. The grating technique might also be useful in remote sensing of flames or combustion processes. The combination of spatial resolution and time resolution can make this method a powerful probe of gas-phase dynamics.

Acknowledgement

This work was supported by the National Science Foundation, grant number DMR79-20380.

References

[1] Lemont and Flynn, Ann. Rev. Phys. Chem. 28 (1977) 261.
[2] M.D. Fayer, Ann. Rev. Phys Chem. 33 (1982) 63.
[3] R G. Brewer and R.L. Shomaker, Phys. Rev. Letters 27 (1971) 631;
R.G. Brewer and A.Z. Genack, Phys. Rev. Letters 36 (1976) 959.
[4] P.R. Berman, T.W. Mossberg and S.R. Hartmann, Phys. Rev. A25 (1982) 2550;
R. Kachyn, T.J. Chen, T.W. Mossberg and S.R Hartmann, Phys. Rev. A25 (1982) 1546;
A.H. Zewail, Accounts Chem. Res. 13 (1980) 360, and references therein.
[5] W. Warren and M.A. Banash, Coherence and quantum optics, Vol. 5 (Plenum Press, New York, 1984) p. 959;
M.A. Banish, J. Gotuw and W.S. Warren, J. Luminescence, to be published.
[6] L.S. Ornstein and W.R. van Wijk, Z. Physik 78 (1932) 734.
[7] R. Vasudev, R.N. Zare and R.N. Dixon, J. Chem. Phys. 80 (1984) 4863.
[8] T.S. Rose, R. Righini and M.D. Fayer, Chem Phys. Letters 106 (1984) 13
[9] J.K. Tyminski, R C. Powell and W.K. Zwicker, Phys. Rev. B29 (1984) 6074.
[10] K.A. Nelson, R. Casalegno, R.J.D Miller and M.D. Fayer, J. Chem. Phys. 77 (1982) 1144.
[11] F.E. Stafford, J. Chem. Ed. 39 (1962) 627.
[12] P. Luc, J. Mol Spectry. 80 (1980) 41.
[13] J. Tellinghuisen, J. Chem. Phys. 76 (1982) 4736.
[14] I.A. Levine, Physical chemistry (McGraw-Hill, New York, 1978) pp. 421, 597, 598.